Ultrathin Layer Cell for Electrochemical and Electron Transfer Measurements

Fu-Ren F. Fan and Allen J. Bard*

Contribution from the Department of Chemistry, University of Texas, Austin, Texas 78712.
Received June 20, 1986

Abstract: An electrochemical cell based on electrodes of near-atomically-smooth platinum on mica surfaces with an interelectrode gap width (r_0) adjustable with piezoelectric drive elements with a resolution of ca. 1 Å for distances of 0 to >500 nm is described. Measurements of the steady-state current for solutions of $Fe(CN)_6^{3-/4-}$ show good agreement with electrochemical thin layer cell equations derived for physical diffusion of species between the electrodes, corrected for the geometry of this cell (crossed hemicylindrical electrodes) for $r_0 \gtrsim 200$ Å. For ca. 10 Å < r_0 < 200 Å at higher concentrations (>2 mM) of electroactive species with small interelectrode potential differences (≤10 mV), the current is larger than predicted; several possibilities for this current enhancement are suggested. Electron transfer from an electroactive polymer film of either reduced *N,N'*-bis-[3-(trimethoxysilyl)propyl]-4,4'-bipyridinum or oxidized poly(vinylferrocene acrylonitrile) to a similar film on the second electrode is also demonstrated.

We describe an electrochemical cell with near-atomically-smooth electrode surfaces and an apparatus to produce adjustable and variable interelectrode spacings of 0 to >500 nm; results of electrochemical measurements with dissolved species and polymer layers are reported. This apparatus was designed to probe homogeneous and heterogeneous electron transfer reactions. Thin layer electrochemical cells, with solution layer thicknesses of 10–100 μm, have been widely used for a variety of electrochemical and spectroelectrochemical experiments.[1] However, cells with much closer electrode spacing (r_0), which we will call ultrathin layer cells (UTLC), encompass a number of new features. The diffusional transit times between electrodes, ca. r_0^2/D, where D is the diffusion coefficient (ca. 10^{-6} cm^2 s^{-1}) and r_0 ca. 10 nm will be $<10^{-6}$ s, so that very rapid chemical reactions can be studied. Moreover, at spacings ≲1 nm direct electron transfer between electrodes (e.g., tunneling or intermolecular transfer between species on the electrode surfaces) becomes possible. In the construction of an UTLC and associated apparatus, one must consider a number of factors: (1) electrodes must be fabricated that are atomically smooth and parallel over the interelectrode contact region; (2) these must be moved with respect to one another with Å-scale resolution; (3) the interelectrode spacing must be determined with similar resolution; (4) thermal drifts and vibration that can affect the spacing must be minimized; (5) the electrode surfaces and solutions must be maintained at a high degree of cleanliness to avoid dust particles and other impurities. In designing this apparatus we used the principles and methodology of the surface forces apparatus[2-4] that has been used to measure the forces between two thin mica sheets attached to crossed hemicylindrical pieces as these are brought together. The details of construction are shown in Figure 1 and are contained in the Experimental Section. Each electrode consists of platinum sputtered on a freshly cleaved mica substrate, which in turn is glued to a hemicylindrical lens. Two such lenses are arranged in a crossed configuration to minimize problems of maintaining the surfaces parallel. They are moved with respect to each other with piezoelectric drives whose movements are calibrated by multiple beam interferometry.[2-5] In the experiments described here, the current that flows between the electrodes as they are brought together is a direct measure of the rate of charge propagation via solution species, of charge transfer between species, on the electrode surfaces, or of electron tunneling between the electrode surfaces. Application of this apparatus to other types of experiments will also be considered.

Experimental Section

Electrode Preparation. The thin platinum films (400–500 Å) on thin mica sheets (1–3 μm) were prepared based on the method reported previously.[6] These Pt-coated mica sheets were then cut into nearly square shapes (ca. 1 cm^2) with a sharp razor blade and glued (Epoxy-30, Transene Co., Rowley, MA) on the surfaces of cylindrical lenses (radius of curvature, ca. 2 cm) with the mica surface facing the lens. Electrical contact was made on Pt at the edge of the lens with conductive silver paint (Acme Chemicals and Insulation, Co., Division of Allied Products, New Haven, CT) which was then covered by epoxy cement. Most of these procedures were carried out in a clean hood (Model CCI 848, Forma Scientific, Division of Mallinckrodt, Marietta, OH). The resistance between two contacts on opposite sides of the Pt/mica square was about 50 Ω.

Chemicals and Electrode Modification. *N,N'*-Bis[3-(trimethoxysilyl)propyl]-4,4'-bipyridinium dibromide (BTPV) was synthesized and purified as described previously.[7,8] Electrodes derivatized with BTPV were prepared by scanning the potential between 0.00 and −0.8 V vs. SCE in an aqueous 0.2 M KCl/0.1 M K_2HPO_4 (pH 8.9) solution containing ca. 3 mM BTPV until the desired coverage was obtained.[7] Poly(vinylferrocene acrylonitrile) (PVFAN) was prepared and electrodeposited on (Pt/mica) electrodes by the method of Peerce et al.[9] All other chemicals were reagent grade and were used without further purification. All aqueous solutions were prepared from a Millipore water reagent system and were filtered through Nylon-66 filters (0.2-μm pore size) (Rainin Instruments Co., Woburn, MA 01801). For air-sensitive compounds, the solution was thoroughly purged with prepurified nitrogen and the cell chamber was kept under an atmosphere of nitrogen during the experiment.

Apparatus and Techniques. Electrochemical measurements were performed with a PAR Model 175 universal programmer, a Model 173 potentiostat, and a Model 179 digital coulometer (Princeton Applied Research Corp., Princeton, NJ). The signal was recorded either on a Soltec Model VP-64325 2-pen X–YY' recorder (Soltec Corp., Sun Valley, CA) or on a Hewlett Packard Model 7045B X–Y recorder. All potentials were referenced to the SCE potential, if a three-electrode or a four-electrode configuration was used.

The apparatus for distance adjustment used in the present study is similar to those used for surface forces measurements[2,3] and is shown in Figure 1. The various components are described in more detail in the caption. The various components are described in more detail in the caption. The apparatus consists of a heavy-duty cylindrical stainless-steel chamber which supports a Pyrex glass cell containing the solution and is mounted onto a stainless-steel top plate, which also supports two rigid arms. The relative motion of these two arms is controlled by a three-

(1) Hubbard, A. T.; Anson, F. C. *Electroanal. Chem.* **1970**, *4*, 129 and references therein.
(2) Israelachvili, J. N.; Adams, G. E. *J. Chem. Soc., Faraday Trans. 1* **1978**, *74*, 975.
(3) Klein, J. *J. Chem. Soc., Faraday Trans. 1* **1983**, *79*, 99.
(4) Israelachvili, J. N. *J. Colloid Interface Sci.* **1973**, *44*, 259.
(5) Tolansky, S. In *Multiple Beam Interferometry of Surfaces and Films*; Oxford Universtiy: London, 1949.
(6) Liu, H.-Y.; Fan, F.-R.; Bard, A. J. *J. Electrochem. Soc.* **1985**, *132*, 2666.
(7) Bookbinder, D. C.; Wrighton, M. S. *J. Electrochem. Soc.* **1983**, *130*, 1080.
(8) Gaudiello, J. G.; Ghosh, P. K.; Bard, A. J. *J. Am. Chem. Soc.* **1985**, *107*, 3027.
(9) Peerce, P. J.; Bard, A. J. *J. Electroanal. Chem.* **1980**, *114*, 89.

0002-7863/87/1509-6262$01.50/0

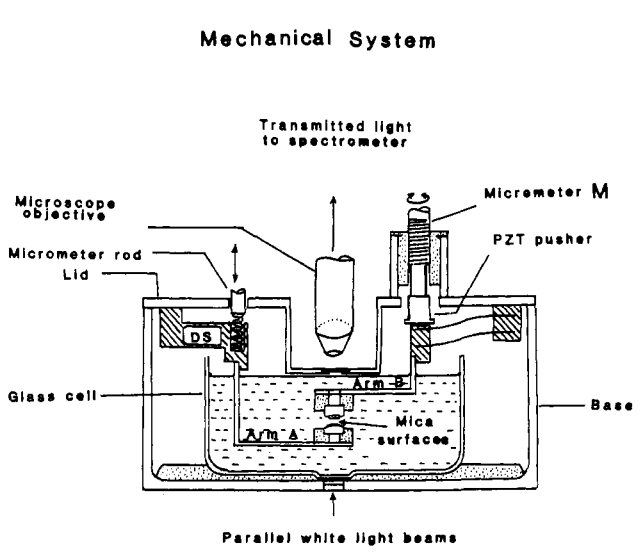

Figure 1. Apparatus for distance adjustment between crossed Pt/mica electrodes. The relative vertical position of the rigid arms A and B, on which cylindrical quartz lenses for Pt/mica sheets are mounted, is controlled via a three-stage mechanism. Coarse adjustment is carried out through micrometer M, on which a piezoelectric (PZT) pusher is attached, with a range of 2–3 mm. A finer adjustment is provided by the differential spring assembly, DS, in which a micrometer-driven rod R pushes a helical spring which in turn acts on a very stiff double-cantilever spring. The ratio of the spring constants of these two springs is ca. 250:1, so that a 1 μm vertical motion of R results in a 40 Å vertical displacement of arm A. The final-stage fine control is through the PZT pusher (Model PZ-30, Burleigh Instruments, Inc., Fishers, NY), which moves arm B vertically up or down, depending upon the voltage applied to the PZT element.

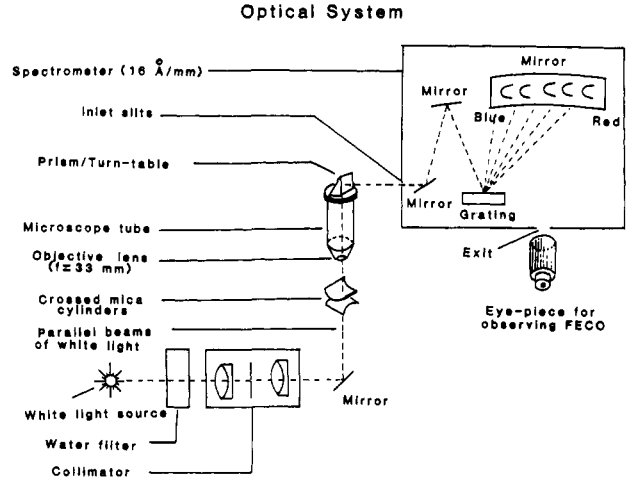

Figure 2. The optical arrangement for white-light multiple-beam interferometry.

stage mechanism consisting of two mechanical stages and one piezoelectric stage, which are mounted on the top plate. The cylindrical quartz lenses with attached Pt-coated mica sheets are mounted onto these two arms in a crossed-cylinder configuration (which minimizes problems of alignment).

The separation between the two Pt surfaces was determined by calibrating the movement of the piezoelectric crystal using white-light multiple-beam interferometry; the basic techniques have been described previously.[4,5] A schematic diagram of this apparatus is shown in Figure 2. White light from a 250-W quartz–halogen lamp, after filtering infrared radiation via a water filter, is passed through a collimator to produce a parallel beam, which is then reflected normally to the pair of Pt-coated mica electrodes by a front surface silvered mirror. In passing through the platinum thin film sandwich, the light undergoes multiple reflections. The transmitted light is focused by a microscope objective (f = 33 mm) and is reflected via a prism/turn-table assembly onto the slit of a spectrometer (Spex, 0.5 m, dispersion 16 Å/min), where a series of fringes (FECO, or fringes of equal chromatic order)[5] are formed and can be viewed by the experimenter through an eye-piece (×10). From the location of the FECO fringes and the refractive index of the medium

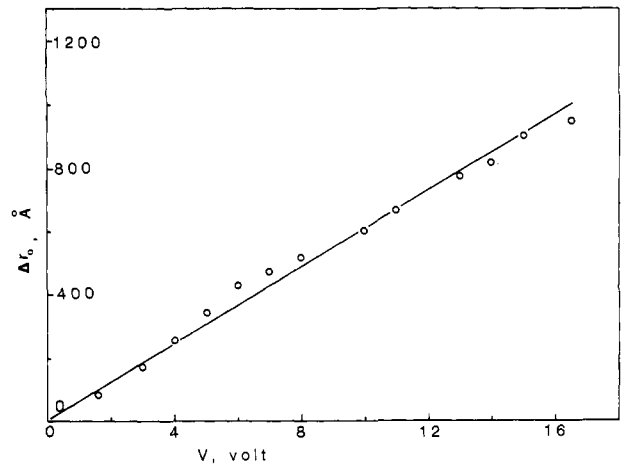

Figure 3. Calibration curve for the displacement of PZT pusher as a function of the applied voltage.

separating the two Pt surfaces, it is possible to evaluate the separation of the surfaces and the change of the separation.[4,5,10] We apply the same technique to calibrate the differential-spring assembly and the piezoelectric pusher. As opposed to measurements with the surface forces apparatus, where the absolute distance between the mica surfaces can be measured by observation of fringes formed by silver films on the mica surfaces facing the hemicylindrical lenses, in our system the fringes result from the Pt films facing the solution. Thus, we can only calibrate our system by measuring the displacement of fringes when the separation between two Pt films, r_0, is 1–3 μm. Figure 3 shows the voltage dependence of the displacement, Δr_0 of the PZT pusher in H_2O when r_0 is ca. 2 μm. It can easily be seen that the linearity is reasonably good over this voltage range; this range (<20 V) was usually used in the electrochemical experiments. The observed deviations from linearity in Figure 3 probably result more from uncertainties in the optical measurements than from deviations from linearity of motion over this voltage range. Note that the manufacturer's specifications indicate a linearity of below ±5% over a range of motion of 5 μm (applied voltage 1000 V); better linearity is expected over a much smaller range of voltage and motion. A slope of 60 ± 5 Å/V was estimated from these measurements; this is close to the value (50 ± 5 Å/V) supplied by the manufacturer of the PZT. In our short-distance experiments the electrodes were positioned ca. 1000 Å apart and then driven toward one another continuously at ca. 1 Å/s. Absolute distance was estimated from the contact point and the above calibration factor. The ratio of the displacement of arm A to that of the micrometer rod R of the differential-spring assembly was 250:1 in the usual operation mode.

Procedure. Before each experiment, the stainless-steel arms and the Delrin lens mounts were ultrasonicated in trichloroethylene and rinsed with EtOH and filtered Millipore water. The cylindrical quartz lenses could be recovered after a series of experiments by ultrasonication in *N,N*-dimethylformamide to remove the mica sheet and glue and then rinsed with alcohol and filtered Millipore reagent water. These components were left to dry in the clean hood.

The cylindrical quartz lenses with (Pt/mica) sheets are mounted on Delrin lens mounts which are mounted on the respective arms A and B. The two Pt surfaces are then ca. 2 mm apart. The base of the stainless-steel chamber, within which the glass cell is resting, is elevated from below to attach to the top plate, which is then screwed tightly onto the base. The whole apparatus rests on three legs with rubber or Viton mounts and is placed on a vibration-isolation optical table (Model RS-510-12/XL4B, Newport Corp., Fountain Valley, CA).

The Pt surfaces are brought together into near contact, and the Newton rings at the contact position are observed through the microscope. Any (Pt/mica) sheet which shows abnormal rings in this preliminary check is discarded. A second check of the Pt/mica electrode is carried out by applying a small voltage (e.g., 10 mV) to the electrodes and monitoring the tunneling current in air. The current through a pair of good Pt/mica electrodes should increase several orders of magnitude with decreasing distance for spacings less than 10 Å. Once a pair of good Pt/mica electrodes is found, the surfaces are then separated and ca. 700 cm^3 of solution is introduced into the cell; this suffices to fill the cell and cover the exit window to the microscope objective. The Pt surfaces are brought together into near contact again and the fringes are observed at

(10) Scott, G. D.; McLauchlan, T. A.; Sennett, R. S. *J. Appl. Phys.* **1950**, *21*, 843.

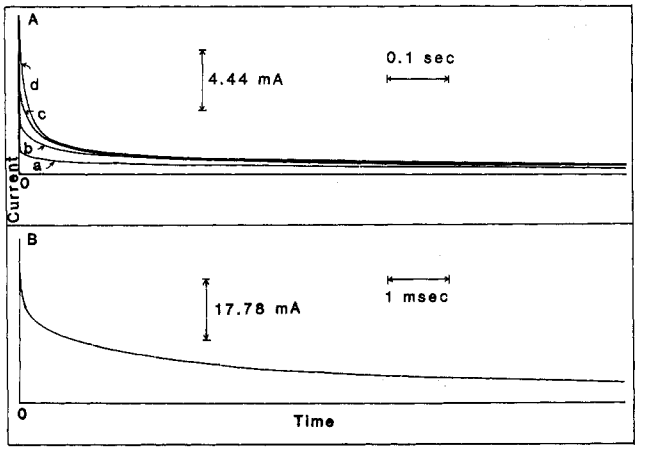

Figure 4. Chronoamperometric curves at different voltage steps and different separation of two electrode surfaces. These experiments were performed as a two-electrode circuit with a 0.5 M aqueous Na_2SO_4 solution containing 4 mM each $Fe(CN)_6^{3-}$ and $Fe(CN)_6^{4-}$. (A) Step-voltage dependence at 5000 Å electrode separation: (a) 0.100 V; (b) 0.236 V; (c) 0.40 V; (d) >0.700 V. (B) Distance dependence with 1.300 V step voltage at 2000, 5000, or 10000 Å.

the contact position. It is at this stage that we detect the presence, if any, of dust particles between the surfaces; only systems free of dust particles and showing normal fringes and current–distance behavior in the absence of an electroactive species are used in further experiments.

After allowing at least 5 h for thermal equilibration with the ambient and mechanical relaxation of the apparatus, electrochemical measurements are performed. For experiments involving short distances (<1000 Å), the instrument is operated by slowly scanning the voltage (ca. 20 mV/s) to the piezoelectric drive element, thus generating a displacement of ca. 1 Å/s.

Results

Voltage Step Experiment. Initial potential step experiments were carried out with $Fe(CN)_6^{3-/4-}$ solutions at different time scales and with different interelectrode spacings to check electrode behavior and judge when the response changes from transient (Cottrell[11]) to steady state. Typical chronoamperometric curves for different voltage steps and different separations between the two electrode surfaces are shown in Figure 4. These experiments were performed in a two-electrode configuration. As shown in Figure 4A, the current (i)–time (t) behavior strongly depended upon the applied step voltage magnitude, when its amplitude was low (<0.5 V). At the current levels of this experiment, the combined resistance of the Pt film and solution are such that resistive drops prevent the potentials at the electrode surfaces from attaining values (within the first ca. 50 ms) where total diffusion-controlled currents are attained. When the step voltage was higher (>0.7 V) and the separation of two electrodes, r_0, was sufficiently large (e.g., ≥5000 Å), the chronoamperometric curves follow Cottrell behavior, i.e., i was proportional to $t^{-1/2}$, over a reasonably wide time window, (see Figure 5). From the slope of the i–$t^{-1/2}$ curve, with an electrode area of 1.15 cm^2, a diffusion coefficient of 7.0×10^{-6} cm^2 s^{-1} was obtained via the Cottrell equation; this agrees well with the reported values for $Fe(CN)_6^{3-/4-}$.[12] At short times (<1 ms) the transient behavior, as expected, is insensitive to the separation of two electrodes, if the two surfaces are not too close [e.g., larger than 2000 Å or $r_0 \gg (\pi Dt)^{1/2}$] (see Figure 4B). At a longer time scale, i.e., when $r_0 \ll (\pi Dt)^{1/2}$, a steady-state current was obtained and the current was substantially larger than that calculated by the Cottrell equation.

Steady-State Current vs. Distance between Two Electrodes. The steady-state current as a function of separation between the two electrodes, in an aqueous solution containing 5 mM $Fe(CN)_6^{3-}$ and 5 mM $Fe(CN)_6^{4-}$ at a bias voltage of 0.236 V is shown in Figure 6. The current was much less dependent upon r_0 than that for a pair of parallel electrodes, where

$$i = nFADC^*/r_0 \quad (1)$$

(C^* is the analytical concentration of electroactive species, F the Faraday constant, and A the electrode area). At large r_0 (>5000 Å), the current increases essentially logarithmically with decreasing r_0. At small r_0 (20 Å < r_0 < 5000 Å), the current was essentially independent of the separation between the two electrodes. The interpretation of this i vs. r_0 relation requires a consideration of the geometry of the two electrodes, i.e., the crossed cylinder arrangement, and the fact that the active electrochemical area effectively decreases as r_0 decreases. We treat the case for a thin layer cell of this geometry in the Appendix. The current is derived by assuming that one-dimensional linear diffusion is applicable to this geometry and that lateral diffusion from the bulk into the thin layer gap during the experiment can be neglected. If the two (Pt/mica) electrodes are treated approximately as two crossed elliptic surfaces glued on cylindrical lenses along axes parallel to individual minor axis of two ellipses, eq 2 describes the steady-state limiting current as a function of the separation between two electrodes:

$$i_l = nFD(\Delta C)g(r_0,h_0,A) \quad (2)$$

in which $g(r_0,h_0,A)$ is a geometric factor and is a function of the closest distance (r_0) between the two electrodes, the maximum effective area (A) of the electrode, and the curvature (h_0) of the cylindrical lens at the edge of the effective area, and is given by

$$g(r_0,h_0,A) = 2A/h_0[1 - (2.303r_0/h_0) \log (1 + h_0/r_0)] \quad (3)$$

The parameters in eq 2 and 3 are defined in the Appendix.

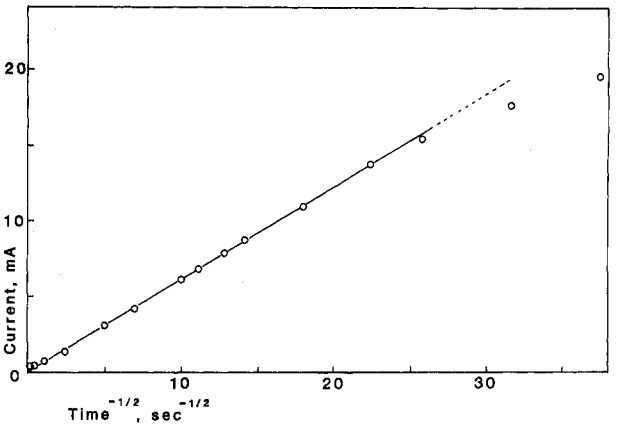

Figure 5. Cottrell plot of limiting behavior of i–t in Figure 4. Electrode separation is 5000 Å and the step voltage is 1.000 V.

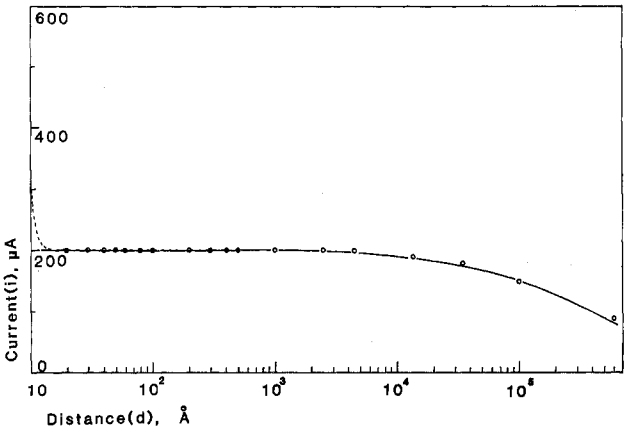

Figure 6. Steady-state current as a function of separation between two electrodes in 0.5 M aqueous Na_2SO_4 solution containing 5 mM each $Fe(CN)_6^{3-/4-}$ at a bias voltage of 0.236 V. Dashed line and circles are experimental results; solid curve shows theoretical calculation based on eq 1 and 2 with $n = 1$, $F = 9.65 \times 10^4$ C/eq; $D = 7.4 \times 10^{-6}$ cm^2/s; $\Delta C = 10^{-5}$ mol/cm^3; $h_0 = 10^{-2}$ cm, and $A = 0.14$ cm^2.

(11) Bard, A. J.; Faulkner, L. F. In *Electrochemical Methods*; Wiley: New York, 1980; p 142.
(12) Zhang, X.; Leddy, J.; Bard, A. J. *J. Am. Chem. Soc.* **1985**, *107*, 3714.

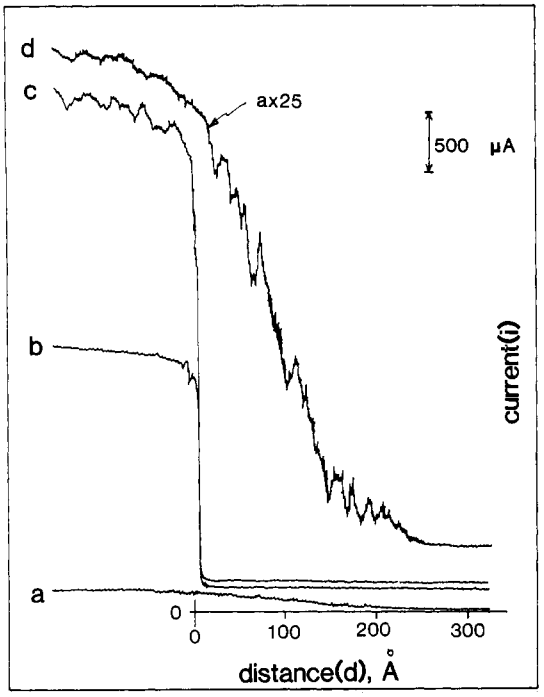

Figure 7. The current–distance relation as a function of bias voltage in 0.5 M aqueous Na_2SO_4 solution containing 5 mM each $Fe(CN)_6^{3-/4-}$: (a) 10 mV; (b) 118 mV; (c) 236 mV; (d) curve a at higher sensitivity.

By taking $n = 1$, $F = 9.65 \times 10^4$ C/equiv, $D = 7.4 \times 10^{-6}$ cm^2/s, $\Delta C = 10^{-5}$ mol/cm^3, and $h_0 = 10^{-2}$ cm, we can fit the experimental results with those calculated based on eq 2 and 3 for distances ranging from 25 to 10^5 Å when A is taken as 0.14 cm^2 (Figure 6). For distances greater than 10^5 Å, the experimental current was slightly higher than that based on theoretical calculation, perhaps because of a significant contribution from a larger active area. Note that when (r_0/h_0) become less than 1.6×10^{-3} the bracketed term in eq 3 is essentially (within 1%) unity and the current is independent of r_0 and given by

$$i_{1,ss} = 2nFD(\Delta C)A/h_0 \qquad (4)$$

In the system here, this occurs for $r_0 < 1600$ Å.

At apparent distances <10 Å the current shows a rapid (essentially exponential) increase with decreasing apparent (as deduced from piezoelectric drive voltage) distance. This increase, which is essentially the same in the presence and absence of electroactive species, can be attributed to several factors, e.g., electron tunneling between the electrodes or interelectrode contact with a varying contact resistance. Because of uncertainties in the distance measurement and electrode smoothness on this scale, we will not discuss measurements in this region any further.

In Figure 7, it is shown that the current–distance relation strongly depends on the applied voltage, especially at very short distances. At contact, shown on the left-hand side of Figure 7, i becomes essentially constant and its magnitude is linearly proportional to the applied voltage. In this region, i is presumably limited by the contact resistance of the Pt thin films. When the concentration of the redox couple is low and the bias voltage is sufficiently large (e.g., >100 mV), i changes from the small electrochemical current to the large contact curent within 10 Å. This sharp feature of the current–distance curves has been used to fix the location of zero distance. At low bias voltage (e.g., 10 mV), the transition between those two conduction regimes becomes much less sharp. Noticeable current was found in the transition region which extends over a wide range of distance between two electrodes (see curves a and d in Figure 7). In addition to the dependence on distance and bias voltage, the current also depends on the concentration of the redox couple as described below.

Dependence of Steady-State Current upon Concentration of Redox Couple. In Figure 8 the concentration dependence of the steady-state current at low bias voltage is shown as a function of distance. The current was recorded under essentially steady-state conditions by scanning the voltage across the piezoelectric element to generate a displacement rate of ca. 1 Å/s. As shown in curve a of Figure 8, in 0.5 M Na_2SO_4 supporting electrolyte alone, no appreciable current was observed until the two electrodes were brought together to within ca. 10 Å, where electron tunneling between the two Pt thin films could take place. As the concentration of the $Fe(CN)_6^{3-/4-}$ couple was progressively increased, the current was essentially proportional to the concentration at larger separations (e.g., ≥400 Å) of the two electrodes (Figure 9b). At smaller separations (e.g., 55 Å), the current was higher than that predicted by eq 2, and its concentration dependence was far beyond linearity (see Figure 9a). Thus, the current–distance behavior, at distances beyond those attributed to tunneling, can be divided into two regions. At longer distances the usual diffusion-controlled thin layer behavior (as modified for geometric factors as in eq 2) applies, but at shorter distances the current is significantly larger than that calculated by eq 2. The width of this "short distance region" depends upon the concentration and nature of the redox couple. The higher the concentration of the redox couple, the wider was the short-distance region (see Figure 8). Similar current–distance behavior was observed for the Fe(II)/Fe(III)–EDTA couple but not for the Cu(II)/Cu(I) couple in a 2 M KCl medium (see Figure 10). Note that for calculations with eq 2 the location for electron transfer to the

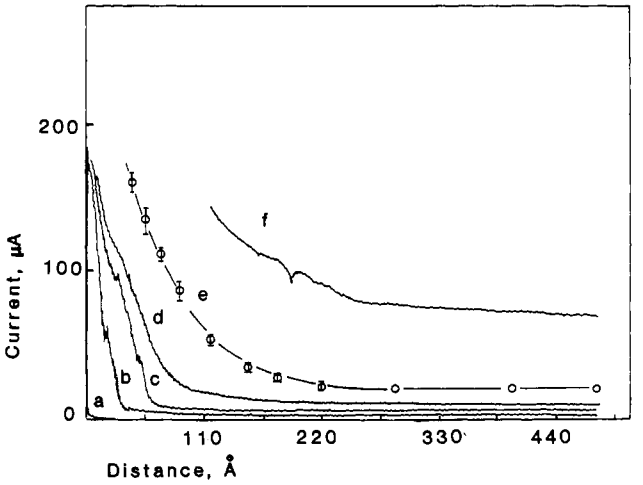

Figure 8. Concentration dependence of the steady-state current at bias voltage of 10 mV and at various distances. The scan rate on PZT pusher was ca. 1 Å/s. Supporting electrolyte, 0.5 M aqueous Na_2SO_4 solution: (a) no $Fe(CN)_6^{3-/4-}$; (b) 0.4 mM each $Fe(CN)_6^{3-/4-}$; (c) 1.0 mM each $Fe(CN)_6^{3-/4-}$; (d) 2.0 mM each $Fe(CN)_6^{3-/4-}$; (e) 5.0 mM each $Fe(CN)_6^{3-/4-}$; (f) 15.0 mM each $Fe(CN)_6^{3-/4-}$.

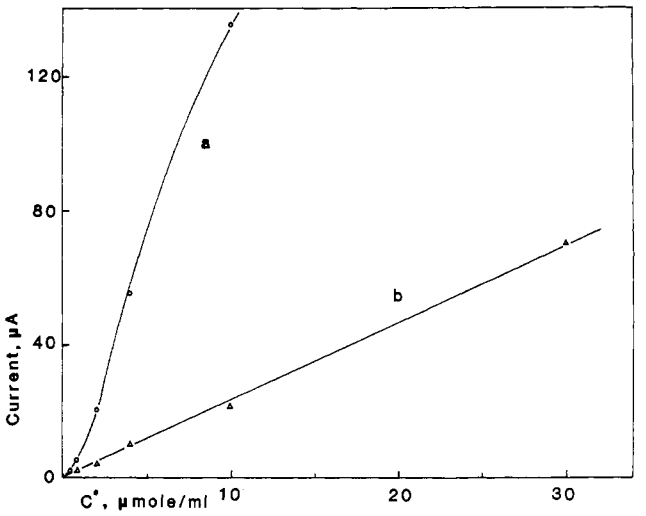

Figure 9. Steady-state current vs. concentration at two electrode separations: (a) $r_0 = 55$ Å; (b) $r_0 = 400$ Å. Data are taken from Figure 8.

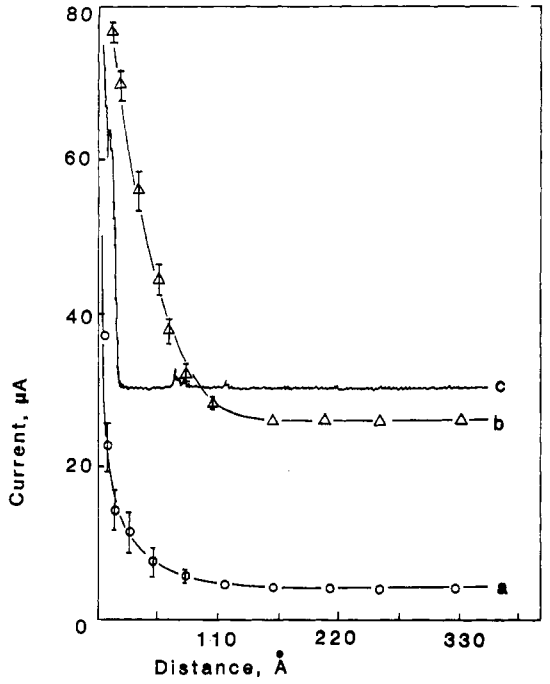

Figure 10. Steady-state current at a bias voltage of 10 mV as a function of the separation between two electrodes for various redox couples: (a) 0.5 mM Fe^{II}–EDTA/2.5 mM Fe^{III}–EDTA in 0.5 M Na_2SO_4; (b) 5 mM each $Fe(CN)_6^{3-/4-}$ in 0.5 M Na_2SO_4; (c) 5 mM each Cu^I/Cu^{II} in 2 M KCl, pH 2.

electrode (usually considered the outer Helmholtz plane) was taken at the Pt surface. The radius of the $Fe(CN)^{3-/4-}$ species is at least 3–4 Å, and may be somewhat larger, if ion-pairing effects are important. However, even assuming that the actual electron transfer distance at both electrodes is ca. 5–6 Å, the currents calculated via eq 2 are much smaller than those observed in the short-distance region.

Polymer Films on (Pt/Mica) Electrodes. We are interested in using this apparatus to measure the rate of electron transfer between a species held on one electrode to a species on the other electrode as a function of distance. In future experiments we hope to carry out electrochemical and spectroscopic measurements on monolayer assemblies or thin films of well-defined thickness on the electrode surfaces. As a first attempt at observing electron transfer between species on the electrode surfaces, we have used polymer modified electrodes.[7,8,13] These studies involve films of electroactive polymers electrodeposited on the surface of the Pt/mica electrodes when each is independently coated in the conventional way.[7,13] In Figure 11, the cyclic voltammograms (CV) of two individual (Pt/mica) electrodes each derivatized with ca. 1000 Å (i.e., 1.05 mC charge or a coverage, Γ, of 3×10^{-8} mol cm^{-2} using the calibration of Bookbinder and Wrighton[7]) of the viologen polymer, BTPV, are shown. The CV was identical with that observed by Bookbinder and Wrighton ($E_{1/2} = -0.55$ V vs. SCE), and the voltammograms at slow scan rates showed thin layer electrochemical behavior; i.e., the peak current is linearly dependent on scan rate. The electrochemical behavior showed, in agreement with the previously reported results,[7] that essentially complete reduction of all the methyl viologen (MV^{2+}) centers in the film occurs. The difference between the anodic and cathodic peak potentials (ΔE_p) was ca. 20 mV, and the width at half-height ($\Delta E_{p/2}$) was ca. 90 mV at a scan rate of 10 mV/s. At a scan rate of 100 mV/s, $\Delta E_{p/2}$ remained 90 mV while ΔE_p increased to ca. 60 mV. These results suggest, in agreement with the ESR results reported by Gaudiello et al.,[8] that the self-exchange rate in these films is rapid and that the films show some resistive effects.

One derivatized Pt/mica electrode was kept at open-circuit and its distance was changed relative to the other derivatized Pt/mica

(13) Murray, R. M. *Electroanal. Chem.* **1984**, *13*, 191 and references therein.

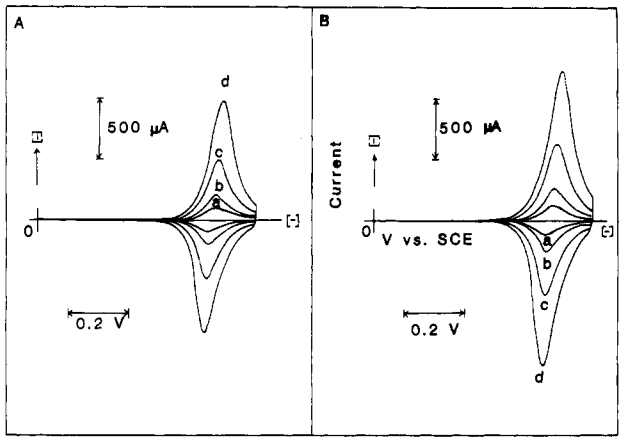

Figure 11. Cyclic voltammograms (CV) of two Pt/mica electrodes (A and B) both derivatized with ca. 1000 Å of BTPV (charge collected for A film is 1.05 mC and that for B film is 1.15 mC) in an aqueous 0.2 M KCl, 0.1 M K_2HPO_4 (pH 8.9) solution. Scan rate: (a) 10 mV/s; (b) 20 mV/s; (c) 50 mV/s; (d) 100 mV/s.

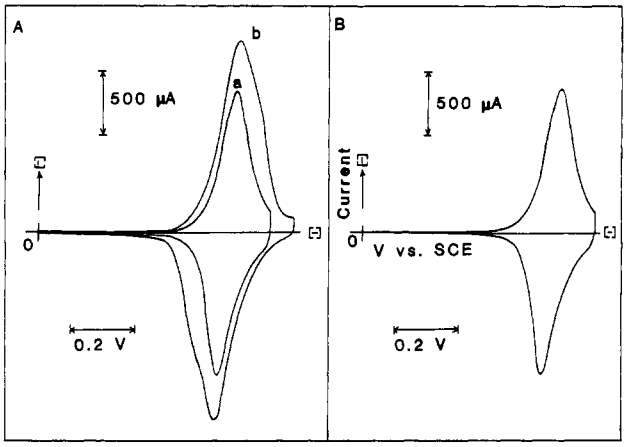

Figure 12. CV on two Pt/mica electrodes each derivatized with ca. 1000 Å of BTPV in an aqueous 0.2 M KCl, 0.1 M K_2HPO_4 (pH 8.4) solution at a scan rate of 100 mV/s. (A-a) One electrode connected and the other at open circuit condition and two electrodes ca. 2 mm apart. (A-b) Same experiment as A-a, but with the two electrodes brought together so that the two Pt films were ca. 2000 Å apart. (B) Same as A-a, after A-b and separation of electrodes.

electrode, which was connected to the potentiostat. Cyclic voltammograms were recorded for various spacings between the electrodes; the results are shown in Figure 12. When the two electrodes were far apart (≥2 mm), only one electrode was electrochemically active (curve a in Figure 12A) and the charge collected during reduction was 1.15 mC. When the two polymer films "contact" one another (separation between two Pt films about 2000 Å), the CV waves increased with a total charge collected during reduction of 2.23 mC, indicating that at this distance both polymer films were electrochemically active (curve b in Figure 12A). After separating the two electrodes (≥2 mm), the CV was nearly identical with the original one (curve a of Figure 12A) with the same charge collected (see Figure 12B). Experiments in which voltammograms were recorded as the electrodes were brought together and then separated could be repeated many times with essentially no change in behavior or indications of removal of polymer film from either electrode.

In Figure 13 is shown the effect of scan rate for the CV of two derivatized Pt/mica electrodes. The voltammograms at slow scan rates (<20 mV/-s) showed thin layer electrochemical behavior. However, both ΔE_p and $\Delta E_{p/2}$ at higher scan rates (>20 mV/s) were larger than those observed for individual polymer films owing to the finite self-exchange rate between and along the films as well as resistive effects of the polymer and Pt films. At slow scan rates (<20 mV/s), $\Delta E_{p/2}$ was still about 90 mV. With increasing scan rate, a clear shoulder could easily be identified at potentials

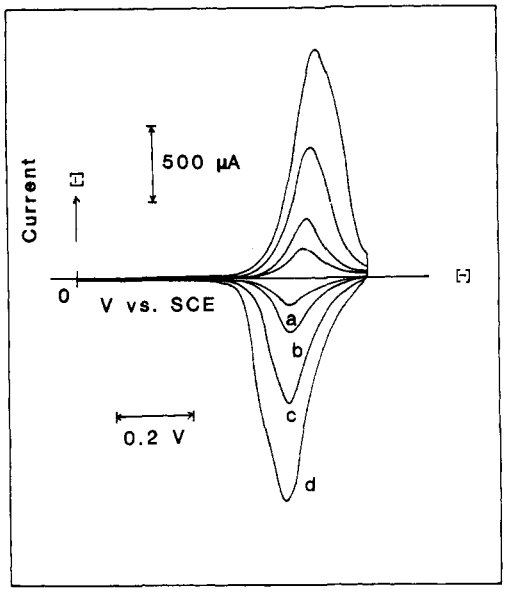

Figure 13. CV of two BTPV-derivatized (Pt/mica) electrodes at ca. 2000 Å separation between the two Pt films in 0.2 M KCl, 0.1 M K_2HPO_4 (pH 8.9) solution. One electrode connected and the other is at open-circuit condition. Scan rate: (a) 10 mV/s; (b) 20 mV/s; (c) 50 mV/s; (d) 100 mV/s.

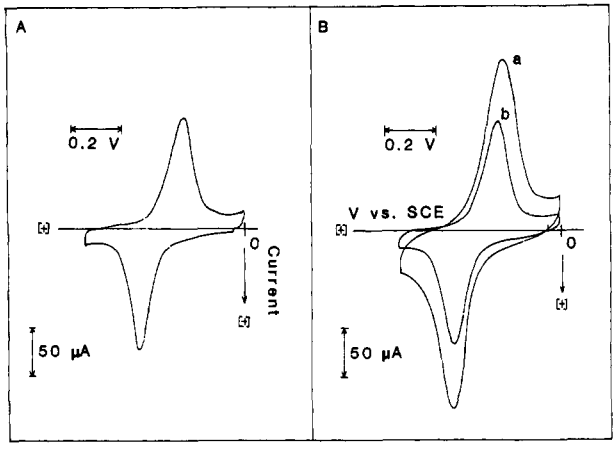

Figure 14. CV on two Pt/mica electrodes each covered with ca. 300 Å of PVFAN in an aqueous 0.5 M $NaClO_4$ solution at a scan rate of 100 mV/s. (A) One electrode connected and the other at open-circuit condition and two electrodes are ca. 2 mm apart. (B-a) Repeat experiment A with two electrodes brought together with the two Pt films ca. 1600 Å apart. (B-b) Repeat experiment A after experiment B-a.

different from the peak potentials.

We have also performed similar experiments with poly(vinylferrocene acrylonitrile) (PVFAN) derivatized electrodes. As shown in curve a of Figure 14B, two PVFAN films (each ca. 300 Å thick, based on the charge collected during electrodeposition), one at open circuit and one driven, showed electroactivity of both films when the separation between the Pt films was ca. 1600 Å. This distance deviates substantially from the total thickness of two polymer films and suggests that in this case the film deposition was not uniform and that thicker islands of PVFAN had formed on the electrode surface.

Discussion

The current–distance behavior can be divided into four zones delimited (roughly) by the interelectrode separation, r_0: contact ($r_0 \leq 0$); tunneling ($0 < r_0 \lesssim 10$ Å); short distance ($10 < r_0 \lesssim 200$ Å); long distance ($r_0 \gtrsim 300$ Å). Measurements in the very short distance region and a clear delineation of tunneling, as opposed to contact resistance effects, require knowledge about the smoothness of the Pt films deposited on mica. Extensive research on cleaved mica with surface forces apparatus and interferometric measurements[2-5] suggest these are atomically smooth over regions of near-contact similar to those employed here. There is less information available about thin Pt films deposited on mica.[6] The films show no distinguishable features by scanning electron microscopy at up to 40 000× magnification. We have performed scanning tunneling microscopy (STM)[14] experiments in air on several Pt-coated mica sheets. As shown in Figure 15, these Pt films are smooth (within 10 Å) in most areas scanned. There are, however, some steps of ca. 50–100 Å that are occasionally detected at some locations on thick films. Recent results reported by Maeda et al.[15] on the characterization of sputtered 10-nm thick Pt films on freshly cleaved mica, prepared in a very similar way to those used here, by direct-phase-detecting microscopic interferometry showed an average roughness of 1 nm over a sampling area of about 0.1 mm^2 with essentially no features greater than ±5 nm. With a radius of curvature of 2 cm, as employed here, the effective area of the electrodes was estimated as 0.14 cm^2 for distances up to 10^4 Å. In the long-distance region the effects of nonuniformities of the order of 1 nm would be averaged out. In the tunneling region such roughness would be of major concern. At this time we can only speculate that one is examining the effects of the closest points at these distances, just as is assumed to be the case in STM.[14] More elaborate and careful experiments are planned using other electrode materials that are atomically smooth (e.g., fresh surfaces on stress-annealed pyrolytic graphite and layered conductive or semiconductive substances, such as WSe_2, MoS_2, TiS_2), or using STM techniques, to examine this region.

The long-distance ($r_0 \gtrsim 300$ Å) steady-state current can be described very well by the usual mass transfer controlled electrochemical approach, eq 2 and 3 (see Figure 6). However, at shorter distances the current appears larger than the essentially constant current predicted by eq 2. We feel this is not simply an effect of geometry or artifact caused by approximations or

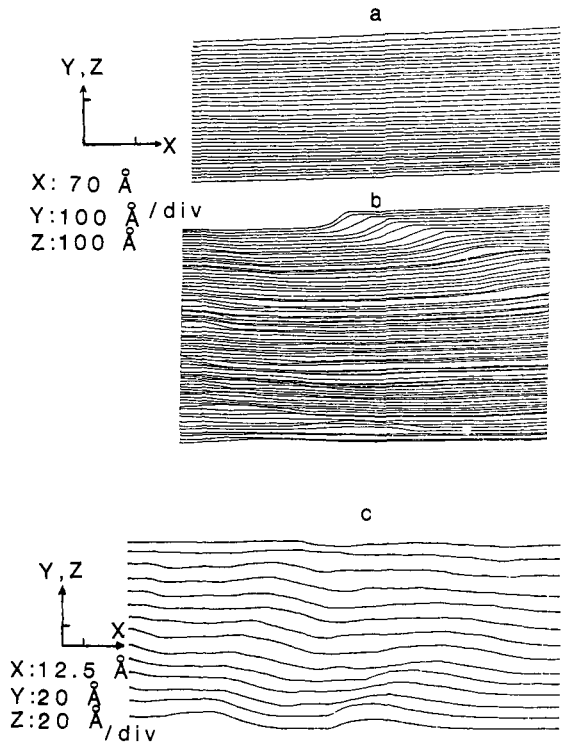

Figure 15. STM image of Pt-coated mica sheets in air. Tunneling current at 0.5 nA; bias voltage at 50 mV between W tip and sample. (a) Pt (1.8 μm)/mica; (b) Pt (1.8 μm)/mica, another location; (c) Pt (500 Å)/mica.

(14) (a) Binnig, G.; Rohrer, H. *Surf. Sci.* **1983**, *126*, 231. (b) The STM employed a W tip and piezoelectric X,Y,Z drives, and followed usual STM practice. Details will be published elsewhere (F.-R. F. Fan; A. J. Bard).

(15) (a) Maeda, M.; White, H. S.; McClure, D. J. *J. Electroanal. Chem.* **1983**, *200*, 383. (b) Smith, C. P.; Maeda, M.; Atanasoska, L.; White, H. S.; McClure, D. J. *J. Phys. Chem.*, submitted for publication.

Scheme I

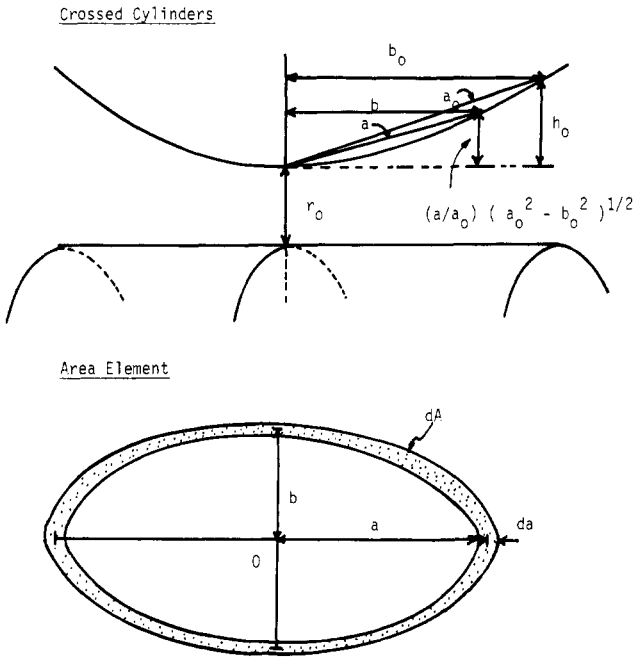

assumptions made in derivation of eq 2, because the magnitude of the "excess current" is a function of solute concentration (Figure 8) and nature of the solution redox species (Figure 10). Moreover, the effect is reproducible in different trials with different electrodes. Several factors might play a role in this current deviation. These include changes in concentration of redox species because of electrostatic attraction (or repulsion) at the electrode surfaces (i.e., diffuse double layer effects), specific electron-hopping or transfer through the solution at short distances, and structuring of the solution by the electrode surfaces. The effect of other phenomena, such as a change in dielectric constant, extended heterogeneous electron transfer processes,[16] a change of viscosity near the electrode surface,[17] and film formation on the electrodes might also be important at very small separations. We are currently attempting to elucidate the possible contribution of these factors.

A second aspect of this work pertains to electron transfer between species held on the electrode surfaces. The first experiments of this type involved polymer films and demonstrated that electron transfer, e.g., from reduced viologen moieties in BTPV on one electrode to unreduced material on the second electrode, can occur. The electrochemical activity of the individual polymer films was maintained after bringing the two films together and performing electrochemical experiments repeatedly. Clearly demonstrated in Figures 12 and 14 is the long-distance electrochemistry in which the electrochemical activity of an electrochemically active polymer film can be controlled by the other film which is physically separated from the first. These results also indicate that the self-exchange rates in these polymer films is high.[7] However, the roughness of the films and the geometry of the electrode prevent us from estimating the self-exchange rate constant and the interfilm electron hopping distance. Experiments with better defined thin films or adsorbed or covalently bound monolayers utilizing electrochemical or photochemical techniques are currently under way.

(16) Feldberg, S. W. *J. Electroanal. Chem.* **1986**, *198*, 1.
(17) See, for example: Chan, D. Y. C.; Horn *J. Chem. Phys.* **1985**, *83*, 5311.

Conclusions

The mica surface forces methodology has been applied to the construction of a new apparatus, an ultrathin layer electrochemical cell, with a gap that can be varied at the Å level. This has been applied to studies of electron transfer to solution redox couples (e.g., $Fe(CN)_6^{3-/4-}$) and polymer films on the electrode surfaces. At high bias voltage and at short distance, the steady-state current is mainly contributed from the central part of the electrode via one-dimensional linear diffusion, while on the wide separation, short time scale, the electrochemically active area is the whole geometric area of the Pt surface. The application of this technique to other problems such as transient electrochemical experiments, electrogenerated chemiluminescence, and photochemistry is underway.

Acknowledgment. We are indebted to Drs. Jacob Israelachvili, Anita Bailey, Paul Luckham, and Stephen Feldberg for helpful advice and suggestions. This work was supported by the Robert A. Welch Foundation, the University of Texas Laboratory for Electrochemistry, and the National Science Foundation (CHE8402135).

Appendix: Derivation of Steady-State Current between Crossed Cylinder Electrodes

For two crossed cylinders, e.g., the Pt/mica attached to hemicylindrical lenses, the figure described by equidistant lines between the cylinders is an ellipse (Scheme I). If r_0 is the shortest distance between the cylinders (at the center of the ellipse), the distance between the two elliptical areas at any distance from the center, a, is given by

$$r = r_0 + (a/a_0)(a_0^2 - b_0^2)^{1/2} \tag{A-1}$$

where a_0 and b_0 are the lengths of the major and minor axes of an arbitrary ellipse that defines the maximum effective interfacial area. The area of any elliptical element at a is

$$dA = (2\pi b_0/a_0)a\,da \tag{A-2}$$

We treat the current between facing pairs of area elements on the ellipses by assuming that one-dimensional linear diffusion applies at steady state with no contributions from diffusion perpendicular to the current paths. Thus, the contribution from an element pair of area dA is[1]

$$di = nFD(\Delta C)\,dA/r \tag{A-3}$$

where n is the number of electrons involved in the electrochemical reaction, F is the Faraday, D is the diffusion coefficient of the species, $\Delta C = C_R^c - C_R^a$ (the concentration difference of the reduced form at the cathode and the anode).

Substituting eq A-1 and A-2 into eq A-3 and integrating over all area elements (from $a = 0$ to $a = a_0$), we obtain

$$i = nFD(\Delta C)g(r_0,h_0,A) \tag{A-4}$$

$$g(r_0,h_0,A) = 2A/h_0[1 - (2.303r_0/h_0)\log(1 + (h_0/r_0))] \tag{A-5}$$

$$h_0 = (a_0^2 - b_0^2)^{1/2} \tag{A-6}$$

$$A = \pi a_0 b_0 \tag{A-7}$$

Geometrically A is the area of the maximum effective elliptical surface of the electrode and h_0 is related to the curvature of the cylindrical lens.